Acute study of interaction among cadmium, calcium, and zinc transport along the rat nephron in vivo

O. Barbier, G. Jacquillet, M. Tauc, P. Poujeol and M. Cougnon

AJP - Renal 287:1067-1075, 2004. First published Jul 27, 2004; doi:10.1152/ajprenal.00120.2004

You might find this additional information useful...

This article cites 33 articles, 13 of which you can access free at:
http://ajprenal.physiology.org/cgi/content/full/287/5/F1067#BIBL

Updated information and services including high-resolution figures, can be found at:
http://ajprenal.physiology.org/cgi/content/full/287/5/F1067

Additional material and information about ***AJP - Renal Physiology*** can be found at:
http://www.the-aps.org/publications/ajprenal

This information is current as of September 8, 2005 .

AJP - Renal Physiology publishes original manuscripts on a broad range of subjects relating to the kidney, urinary tract, and their respective cells and vasculature, as well as to the control of body fluid volume and composition. It is published 12 times a year (monthly) by the American Physiological Society, 9650 Rockville Pike, Bethesda MD 20814-3991. Copyright © 2005 by the American Physiological Society. ISSN: 0363-6127, ESSN: 1522-1466. Visit our website at http://www.the-aps.org/.

American Journal of Physiology – Renal Physiology

Downloaded from ajprenal.physiology.org on September 8, 2005

Am J Physiol Renal Physiol 287: F1067–F1075, 2004.
First published July 27, 2004; doi:10.1152/ajprenal.00120.2004.

Acute study of interaction among cadmium, calcium, and zinc transport along the rat nephron in vivo

O. Barbier, G. Jacquillet, M. Tauc, P. Poujeol, and M. Cougnon

Unité Mixte de Recherche-Centre National de la Recherche Scientifique 6548, Université de Nice-Sophia Antipolis, 06108 Nice Cedex 2, France

Submitted 5 April 2004; accepted in final form 22 July 2004

Barbier, O., G. Jacquillet, M. Tauc, P. Poujeol, and M. Cougnon. Acute study of interaction among cadmium, calcium, and zinc transport along the rat nephron in vivo. *Am J Physiol Renal Physiol* 287: F1067–F1075, 2004. First published July 27, 2004; doi:10.1152/ajprenal.00120.2004.—This study investigates the effect in rats of acute $CdCl_2$ (5 μM) intoxication on renal function and characterizes the transport of Ca^{2+}, Cd^{2+}, and Zn^{2+} in the proximal tubule (PT), loop of Henle (LH), and terminal segments of the nephron (DT) using whole kidney clearance and nephron microinjection techniques. Acute Cd^{2+} injection resulted in renal losses of Na^+, K^+, Ca^{2+}, Mg^{2+}, PO_4^{-2}, and water, but the glomerular filtration rate remained stable. ^{45}Ca microinjections showed that Ca^{2+} permeability in the DT was strongly inhibited by Cd^{2+} (20 μM), Gd^{3+} (100 μM), and La^{3+} (1 mM), whereas nifedipine (20 μM) had no effect. ^{109}Cd and $^{65}Zn^{2+}$ microinjections showed that each segment of nephron was permeable to these metals. In the PT, 95% of injected amounts of ^{109}Cd were taken up. ^{109}Cd fluxes were inhibited by Gd^{3+} (90 μM), Co^{2+} (100 μM), and Fe^{2+} (100 μM) in all nephron segments. Bumetanide (50 μM) only inhibited ^{109}Cd fluxes in LH; Zn^{2+} (50 and 500 μM) inhibited transport of ^{109}Cd in DT. In conclusion, these results indicate that *1*) the renal effects of acute Cd^{2+} intoxication are suggestive of proximal tubulopathy; *2*) Cd^{2+} inhibits Ca^{2+} reabsorption possibly through the epithelial Ca^{2+} channel in the DT, and this blockade could account for the hypercalciuria associated with Cd^{2+} intoxication; *3*) the PT is the major site of Cd^{2+} reabsorption; *4*) the paracellular pathway and DMT1 could be involved in Cd^{2+} reabsorption along the LH; *5*) DMT1 may be one of the major transporters of Cd^{2+} in the DT; and *6*) Zn^{2+} is taken up along each part of the nephron and its transport in the terminal segments could occur via DMT1.

heavy metals; epithelial calcium channel; divalent metal transporter 1; kidney

CADMIUM (Cd^{2+}) IS ONE OF THE most commonly found toxic metals present in our environment. The major sources of exposure to Cd^{2+} are contaminated food and water, tobacco, and industrial fumes and dusts (16). Cd^{2+} accumulates in the body, and chronic exposure causes severe nephrotoxicity in humans (16) and animals (2, 4). The renal dysfunction may be due to proximal tubular damage affecting the passive paracellular pathway (14, 27) and decreasing active transcellular ion transport (30). With the use of in vitro models, deleterious effects of Cd^{2+} have been described on several solute transporters, such as stretch-activated ion channels (24), the epithelial Ca^{2+} channel (ECaC) transporter (32), the NaPi-II transporter (19), the Na/glucose transporter (1), and the NaSi-1 transporter (25). These acute effects of Cd^{2+} suggest the involvement of ion transporters in Cd^{2+}-induced nephropathy. Therefore, the question arises as to whether these transporters are affected in vivo after Cd^{2+} exposure. To answer this question, studies have been performed in animal models chronically intoxicated with Cd^{2+} (22, 31). Unfortunately, severe intoxication induces renal solute wasting, as well as nephrotoxic damage to glomeruli and proximal tubular structures, which could mask more subtle alterations in transporter function.

It has been clearly demonstrated that free cytosolic Cd^{2+} is responsible for the toxicological damage to cells and that the bound form of Cd, complexed with proteins like albumin and metallothionein, plays a protective role (8). Cd^{2+} increases urine Ca^{2+} excretion (28), which can affect bone metabolism and cause severe bone pathology (29). A blockade of the distal Ca^{2+} transporter (ECaC) was proposed to explain Cd^{2+}-induced hypercalciuria and associated renal stone formation (26). In light of these findings, it is evident that Cd^{2+} may interact with several different transporters. Such interactions suggest the participation of pathways for free Cd^{2+} reabsorption. Therefore, the free ionized Cd^{2+} might be, with CdMT, Cd-GSH, and Cys-Cd, one of the reabsorbed forms of Cd. Although the uptake of free Cd^{2+} accounts for a minor portion of cellular Cd^{2+} uptake in vivo, it could be of interest to identify the transporters involved because the Cd^{2+} complexed to small peptides may be released at the brush border and then taken up as a free ion by renal cells (27). For this purpose, we have chosen to use acute perfusion of Cd^{2+} and microinjections of ^{109}Cd to study the renal handling of Cd. These protocols minimized the participation of bound Cd forms in Cd reabsorption because the de novo metallothionein or glutathione synthesis induced by Cd^{2+} takes several hours and very little Cd^{2+}-albumin complexes are present in the tubular fluid.

Initial data were reported by Felley-Bosco and Diezi (9). Using in vivo micropuncture and microinjection techniques in the rat, these authors showed that Cd^{2+} was mainly reabsorbed in the proximal tubule and that a sodium-cysteine cotransporter was involved. Since their study, a divalent metal transporter (DMT1) has been cloned (18) and immunolocalized to the apical membrane of the thick ascending limb (TAL), distal tubule (DT), and the cortical collecting tubule (CCT) of the rat nephron (11), suggesting a role for this transporter in the renal handling of divalent metal cations. In a recent study, Wareing et al. (34) have clearly demonstrated in the rat that DMT1 can transport Fe^{2+} along the loop of Henle (LH) and distal tubule. Besides Fe^{2+}, DMT1 also transports Cd^{2+} and Zn^{2+} (18). In

Address for reprint requests and other correspondence: P. Poujeol, UMR-CNRS 6548, Bâtiment Sciences Naturelles, Université de Nice-Sophia Antipolis, Parc Valrose, 06108 Nice Cedex 2, France (E-mail: poujeol@unice.fr).

The costs of publication of this article were defrayed in part by the payment of page charges. The article must therefore be hereby marked "*advertisement*" in accordance with 18 U.S.C. Section 1734 solely to indicate this fact.

0363-6127/04 $5.00 Copyright © 2004 the American Physiological Society

American Journal of Physiology – Renal Physiology

Downloaded from ajprenal.physiology.org on September 8, 2005

view of these findings, we decided to re-investigate Cd^{2+} transport along the rat nephron and its relationship to other cations.

MATERIALS AND METHODS

Three types of experimental techniques were used: clearance, tracer microinjection, and micropuncture. The experiments were carried out in female Wistar rats weighing 180–220 g. The animals were fed a standard laboratory diet. They had free access to water until the start of the experiment and were starved for 18 h before the surgical procedure. Anesthesia was induced by injection of pentobarbital sodium (Nembutal, 5 mg/100 g body wt ip) and maintained by additional 1-mg doses administered when necessary. The animals were then placed on a heated table to maintain their body temperature between 37 and 39°C. A tracheotomy was performed leaving the thyroid gland untouched. One catheter (PE-20) was inserted into the right jugular vein for perfusion of experimental solutions and another (PE-10) into the left ureter for urine collection. For clearance experiments, a third catheter (PE-50) was inserted into the right femoral artery for blood sampling and arterial blood pressure recording (Research BP Transducer, Harvard Apparatus). For tracer microinjection experiments, the kidney was ventrally exposed as described by Gottschalk and Mylle (14). The use of animals was in accordance with the ILAR Guide for Care and Use of Laboratory Animals.

Clearance Experiments

These experiments were performed to analyze the effect of an acute load of Cd^{2+} on whole kidney function. Because it is necessary to induce diuresis when microinjection techniques are used, it was important to determine the effect of Cd^{2+} under the chosen diuretic conditions. Therefore, clearance experiments were carried out in rats intravenously (iv) infused with a 2% NaCl solution at a rate of 100 μl/min. [^{3}H]metoxy-inulin (0.53 Ci/mmol) was used to measure the glomerular filtration rate (GFR). Urine samples were collected serially every 10 min, and blood samples were taken halfway through each urine collection. In all experiments a loading dose of [^{3}H]inulin (4 μCi) was given iv, followed by a continuous infusion of 0.4 μCi/min for the duration of each experiment. Urine collection began 1 h after the administration of the [^{3}H]inulin priming dose. After three control clearance periods, Cd^{2+} was added and infused continuously at a rate of 880 μM/min to maintain a plasma concentration of ~5 μM. After a 40-min equilibration period, urine was collected during three additional 10-min clearance periods.

Tracer Microinjections

Droplets of isotonic buffered solutions containing traces of [^{3}H]inulin and the radioactive isotope of the divalent metal ion under investigation were prepared for injection into early proximal, late proximal, early distal, or late DT sites. The volume injected was 3 nl, and the duration of the injection ranged between 20 and 90 s. The method used to identify the structure was identical to that reported previously (21). Briefly, the tubule segment was selected from its shape, location, and refringence and identified by injecting a small volume (~2 nl of isotonic NaCl solution colored with 0.05% of erioglaucine dye) just before the microinjection. At the start of each microinjection, four 60-s, three 1-min, and two 2-min urine samples were collected serially directly into counting vials containing 2 ml of scintillant. This was followed by a 2-min urine collection to determine the urine flow rate. The amount of injected radioactivity was measured by counting the radioactivity of the injected droplet. Background in the urine was calculated from the activity of the urine samples collected just before each microinjection. Urine recovery for each tracer was expressed as a percentage of the amount injected. This amount in the urine reflects reabsorption of the tracer in all downstream segments.

Control of Injection Site

To ensure that the chosen microinjection site was reproducible from one tubule to another, we have performed parallel micropuncture experiments to measure the F/P inulin at the injection site. Diuretic rats were continuously infused with [^{3}H]inulin (3 μCi/min), and, after a 1-h equilibration period, tubular fluid was collected for 1–2 min in proximal and distal tubules identified as described above.

Late Proximal Micropunctures

The protocol of [^{3}H]inulin infusion and the method used to identified the structure were the same as that for the microinjection technique. Late proximal tubular fluid samples were collected. under free-flow conditions. Each collection lasted 60–120 s. Three successive 30-min clearance periods were performed to determine [^{3}H]inulin and Cd^{2+} concentrations in urine and plasma. Ultrafiltrable plasma Cd^{2+} concentration was estimated by measuring Cd^{2+} after the plasma was spun through a 30-kDa filter (Centrifree micropartition system; Amicon).

Analytic Procedure

^{3}H, ^{109}Cd, ^{45}Ca, and ^{65}Zn radioactivities were measured by liquid scintillation counting (Packard). In plasma and urine samples, Na^+, K^+, Mg^{2+}, Ca^{2+}, Cl^-, and P_i concentrations were determined by ion exchange chromatography (AS50/BioLC, Dionex), and Cd^{2+} was measured by atomic absorption spectrometry using a Zeeman furnace system (Solaar 969, Thermo Optek).

Student's *t*-test was used for statistical analysis. The data are expressed as means ± SE. $P < 0.05$ was considered significant.

Radioactive Material

All radioactive elements were produced by Amersham Pharmacia Biotech UK: [^{3}H]inulin (TRA324), specific radioactivity 120 μCi/mg inulin; calcium-45 (CES.3), specific radioactivity 5–50 mCi/mg ^{45}Ca; cadmium-109 (CUS.1), specific radioactivity 50–1,000 μCi/μg ^{109}Cd; and zinc-65 (ZAS.2), specific radioactivity 83 μCi/mg ^{65}Zn.

RESULTS

Clearance Experiments

The effect of an acute load of Cd^{2+} on whole kidney function was assessed using the clearance technique. Arterial blood pressure was similar during the control and Cd^{2+} infusions (126.2 ± 0.5 and 128.5 ± 4.4 mmHg, respectively; $P > 0.05$, $n = 8$). Sham-treated animals did not show any significant changes over time in plasma Na^+, K^+, Ca^{2+}, Cl^-, or PO_4^{-2} concentrations, whereas plasma Mg^{2+} concentration decreased slightly during the saline infusion (Fig. 1). Concomitantly, urine flow rate, GFR, and electrolyte fractional excretion (FE) remained stable (Fig. 2). In experimental animals, the infusion of Cd^{2+} increased plasma Cd^{2+} concentration to 3.03 ± 0.32 μM and was associated with a significant fall in plasma Ca^{2+}, Mg^{2+}, K^+, Na^+, and PO_4^{-2} concentrations (Fig. 1); although urine flow rate increased and GFR was unchanged (Fig. 2). Furthermore, Cd^{2+} infusion induced significant increases in the FE of Ca^{2+}, Mg^{2+}, K^+, Na^+, Cl^-, and PO_4^{-2} (Fig. 2); most of the filtered Cd^{2+} was reabsorbed by the kidney (FE = 0.0018 ± 0.0005%, $n = 15$).

Tracer Microinjection Experiments

First, as shown in Fig. 3*A*, there was a correlation between the F/P inulin values and the injection site, indicating that the morphological criteria used to estimate the injection site did

American Journal of Physiology – Renal Physiology

Downloaded from ajprenal.physiology.org on September 8, 2005

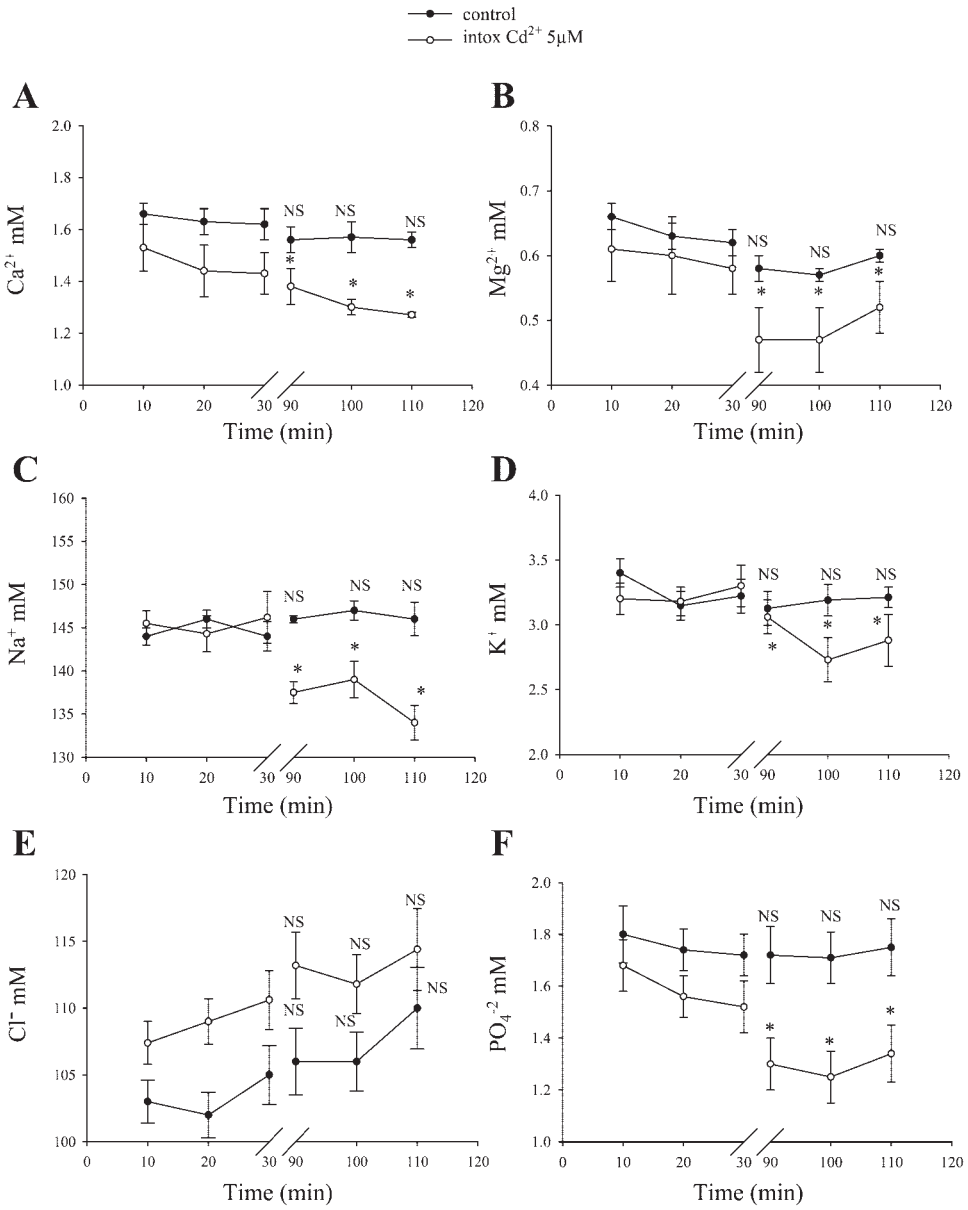

Fig. 1. Effects of 5 μM Cd^{2+} infusion on plasma concentration of Ca^{2+}, Mg^{2+}, Na^+, K^+, Cl^-, and PO_4^{-2} (expressed in mM) in Wistar rats. ●, Control rats ($n = 5$); ○, experimental rats ($n = 5$) exposed to Cd^{2+} throughout the 30-min period; NS, not significant. *Time 0* corresponds to the start of the first urine collection period after 1 h of equilibration. Values are means ± SE calculated for each clearance period. intox, Intoxication. *Difference in the change in plasma concentration between periods without and with Cd by Student's *t*-test ($P < 0.05$).

identify the tubular segment appropriately. Furthermore, in all experiments no site of injection modified the [^{3}H]inulin urine recovery, which was similar to the amount injected (Table 1; see Tables 3 and 4). In a separate series ($n = 3$, Fig. 3*B*), we evaluated nonspecific binding of the tracer to plasma membranes. No change in urine recovery of radioactivity from background occurred after the perfusion of a high concentration of the nonradioactive ion after ^{109}Cd or ^{45}Ca microinjection.

^{45}Ca. Because it has been postulated that Cd^{2+} may affect Ca^{2+} reabsorption, it was first necessary to investigate the tubular transport of Ca^{2+} in the different nephron segments. Results of ^{45}Ca microinjections are shown in Table 1. Ca^{2+} concentration of the injected solution was 4.5 μM. In this experimental series, the Ca^{2+} injection rate ranged between 1 and 3 pmol/min, indicating that Ca^{2+} was introduced into the tubular lumen at tracer doses, because from free-flow micropuncture studies it can be calculated that the mean flow rate of Ca^{2+} varies from 80 pmol/min at the beginning of the proximal tubule to 15 pmol/min at the end of the DT in rats (30). In our experiments, the total amount of Ca^{2+} injected did not significantly increase the normal free-flow delivery rate of Ca^{2+} to the segment located downstream of the injection site, because no significant correlation between the injection rate and the ^{45}Ca recoveries has been found and the cumulative curves of [^{3}H]inulin and ^{45}Ca excretions show that both isotopes appeared in urine and reached their maximum excretion in parallel (data not shown). Table 1 shows that recovery of ^{45}Ca, expressed as a percentage of ^{45}Ca microinjected, depended on the injection site: the more proximal the injection, the lower the ^{45}Ca urine recovery. The differences between the ^{45}Ca recovery at each microinjection site allow an estimate of the unidirectional ^{45}Ca fluxes (expressed as percent delivered load) and provide a measure of Ca^{2+} reabsorption occurring between the early and late proximal tubules, the late proximal and early DTs (including the LH), the early and late DT

American Journal of Physiology – Renal Physiology

Downloaded from ajprenal.physiology.org on September 8, 2005

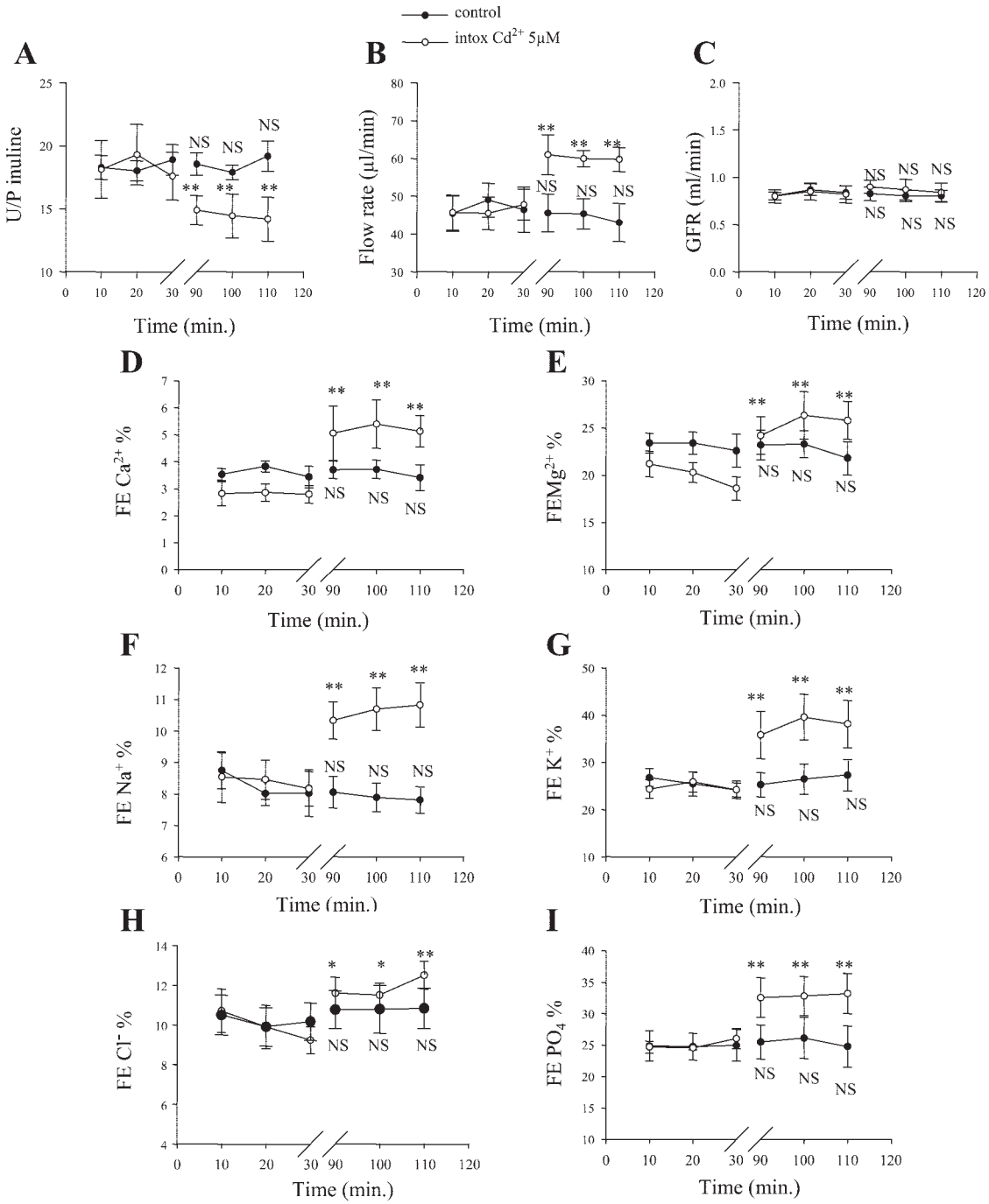

Fig. 2. Effects of 5 μM Cd^{2+} infusion on glomerular filtration (expressed in ml/min), U/P inulin, urine flow rate (expressed in μl/min), and fractionnal excretions (FE) of Ca^{2+}, Mg^{2+}, Na^{+}, K^{+}, Cl^{-}, and PO_4^{-2} (expressed %) in Wistar rats during mild diuretic conditions. ●, Control rats ($n = 5$); ○, experimental rats ($n = 5$) exposed to Cd^{2+} throughout the 30-min period. *Time 0* corresponds to the start of the first urine collection period after 1 h of equilibration. Values are means ± SE calculated for each clearance period, refer to the difference in the change in glomerular filtration rate (GFR), U/P inulin, urine flow rate, and fractional excretions between periods without and with Cd^{2+} by Student's *t*-test (*$P < 0.05$, **$P < 0.001$).

[corresponding to the distal convoluted tubule (DCT)], and the late DT and final urine [including the connecting tubule (CNT) and the convoluted tubule (CT)]. This mode of calculation is valid for calcium because injected ^{45}Ca was in a tracer-dose condition and because a sufficient load of filtered Ca^{2+} was delivered to each segment downstream of the proximal tubule. Under control conditions, >65% of the injected Ca^{2+} was reabsorbed between the late proximal and the early DT, whereas >20% was reabsorbed between the early and late DTs (Tables 1 and 2). The addition of Cd^{2+} (20 μM), Gd^{3+} (100 μM), or La^{3+} (1 mM) significantly increased ^{45}Ca urine recovery when microinjections were performed at the early proximal tubule site (Table1). This increase was mainly due to a decrease in unidirectional ^{45}Ca flux between the early and

American Journal of Physiology – Renal Physiology

Downloaded from ajprenal.physiology.org on September 8, 2005

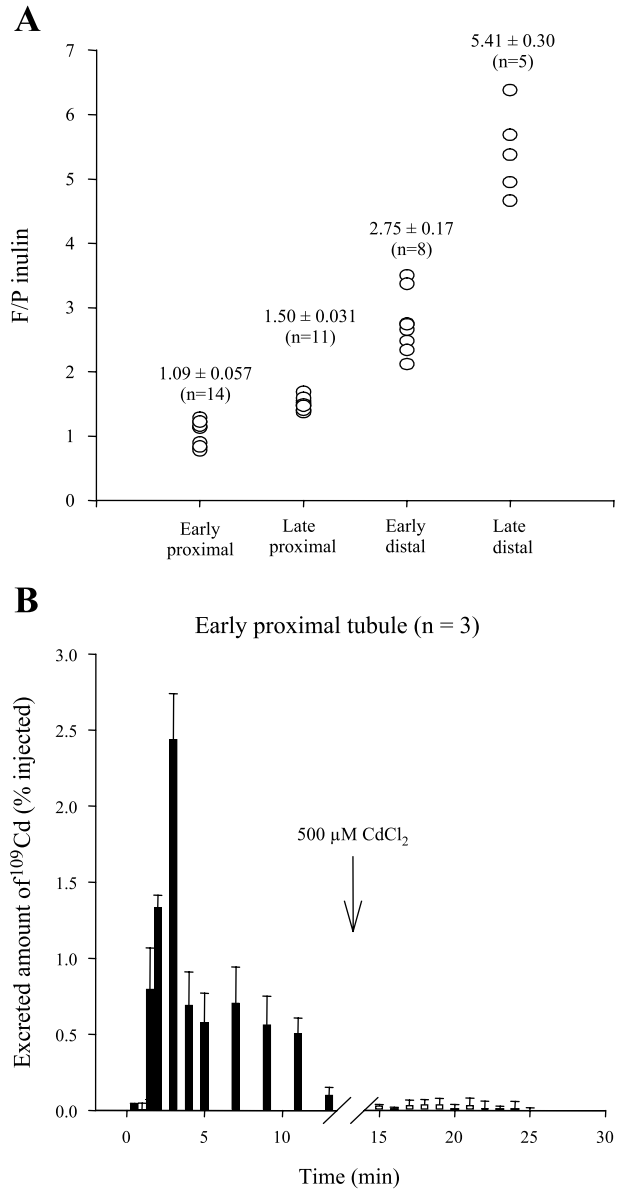

Fig. 3. Correlation between the identification of injected tubules at the kidney surface and the value of F/P inulin (*A*). Measurement of nonspecific binding of cadmium (Cd). A microinjection of ^{109}Cd was performed in early proximal tubule followed by perfusion (arrow) at the same site of 500 μM $CdCl_2$ (*B*). Values are means ± SE. The nos. of microinjections are in parentheses.

late distal segments (Table 2). In contrast, nifedipine did not modify ^{45}Ca recovery at each injection site (Tables 1 and 2). The percent inhibition of distal ^{45}Ca reabsorption produced by each agent used is shown in Fig. 4.

^{109}Cd. The same concentration of Cd^{2+} (5 μM) was used as for a clearance study. This concentration corresponded to that determined during mild chronic exposure (36, 38). The absence of a significant correlation between the Cd^{2+} injection rates and urine recovery (data not shown) has been verified, indicating that under these conditions, the percentage of urine ^{109}Cd recovery reflected Cd^{2+} unidirectional reabsorption. The urine excretion profiles of [^{3}H]inulin and ^{109}Cd were roughly parallel (data not shown) at the three injection sites. Table 3 shows that the urine ^{109}Cd recovery after early proximal microinjection was close to 5% of the amount injected, indicating an important transport of Cd^{2+} in segments beyond this site. The ^{109}Cd excretion was greater when the injections were performed in late proximal and early DTs. Using Cd^{2+} concentrations ranging between 0.005 and 50 mM, microinjections indicate saturation at high Cd^{2+} concentrations in each segment (Fig. 5). These results showed that the segment between early and late proximal sites exhibited an important reabsorptive capacity for Cd^{2+} because in the presence of 50 mM Cd^{2+}, 45% of Cd is reabsorbed. In contrast, the DT exhibited a lower reabsorptive capacity because 5 mM Cd^{2+} is sufficient to saturate the uptake in this segment. To characterize further the transport mechanisms involved in ^{109}Cd fluxes, microinjections were performed in the presence of different cations (Table 3). Unfortunately, in contrast to calcium, the difference between the ^{109}Cd recovery at each microinjection site could not be used to estimate the unidirectional ^{109}Cd in each segment of the nephron flux. This is due to the fact that ^{109}Cd microinjections were not performed in the tracer-dose condition (an endogenous pool of Cd^{2+} does not exist) and because most of Cd^{2+} was taken up by the proximal tubule (see micropuncture results below) so that the amount of ^{109}Cd delivered to the downstream segments after early proximal microinjection was too low to allow mathematical calculation performed for calcium. Therefore, the results were interpreted on the basis of ^{109}Cd urinary recovery after microinjection in early proximal, late proximal, and early DT, respectively. In early, late proximal, and early distal microinjections, the addition of Gd^{3+} (90 μM), Co^{2+} (100 μM), or Fe^{2+} (100 μM) induced a strong increase in ^{109}Cd urine excretion. These data are consistent with a decrease in unidirectional ^{109}Cd fluxes in proximal tubule, LH, and terminal nephron segments (Table 3). The effect of Zn^{2+} is more complicated, because it clearly depends on the concentration used: at a low concentration (50 μM), the addition of Zn^{2+} increased ^{109}Cd excretion only in early distal injections; at a high concentration (500 μM), Zn^{2+} enhanced ^{109}Cd excretion at every injected site. The diuretic bumetanide had an effect only at late proximal sites, suggesting that blockade of the Na^+-K^+-$2Cl^-$ transporter in the LH induces a decrease in ^{109}Cd transport in this segment (Table 3).

^{65}Zn. As for ^{45}Ca and ^{109}Cd, ^{65}Zn microinjections were performed in early, late proximal, and early DTs. With the specific radioactivity of ^{65}Zn available commercially, the minimal concentration in the microinjected solution ranged between 17 and 34 μM, which is higher than the plasma free Zn^{2+} concentration (15 μM). The absence of a positive correlation between the injection rate and ^{65}Zn urine recovery satisfies tracer-dose requirements (data not shown). As shown in Table 4, ^{65}Zn urine excretion increased from early proximal to early distal microinjection sites, indicating significant Zn^{2+} reabsorption along the proximal tubule, LH, and terminal nephron segments. ^{65}Zn microinjections performed in the presence of 50 μM Cd^{2+} showed a slight inhibitory effect of Cd^{2+} on zinc transport along the early proximal tubule and the LH (Table 4). These results also indicate an important inhition of ^{65}Zn transport along the terminal segments of the nephron.

Cd Micropuncture Experiments

Micropuncture experiments were performed to investigate the amount of Cd delivered to the late proximal tubule during

American Journal of Physiology – Renal Physiology

Downloaded from ajprenal.physiology.org on September 8, 2005

Table 1. *^{45}Ca recovery in urine after microinjection along the nephron*

	Control	+Cadmium (20 μM)	+Gadolinium (100 μM)	+Lanthanum (1 mM)	+Nifedipine (20 μM)
			Early proximal		
%^{45}Ca	3.4±0.5 (n = 8)	14.1±1.3 (n = 18; P<0.001)	11.0±1.4 (n = 21; P<0.001)	8.5±0.7 (n = 17; P<0.001)	6.9±1.1 (n = 13; P<0.01)
%[^{3}H]inulin	95.0±2.4	98.8±1.7	99.3±0.4	96.5±1.1	96.5±1.3
			Late proximal		
%^{45}Ca	6.7±1.0 (n = 7)	17.7±1.5 (n = 22; P<0.001)	14.5±2.5 (n = 9; P<0.02)	10.8±0.7 (n = 10; P<0.01)	9.5±1.1 (n = 15; NS)
%[^{3}H]inulin	98.7±1.3	99.3±1.4	98.4±0.8	98.6±0.5	97.7±1.0
			Early distal		
%^{45}Ca	72.8±2.9 (n = 15)	89.5±2.8 (n = 17; P<0.001)	95.9±1.5 (n = 14; P<0.001)	84.3±2.3 (n = 17; P<0.01)	71.4±7.5 (n = 4; NS)
%[^{3}H]inulin	96.3±1.0	100.0±0.5	93.7±1.4	99.3±0.2	97.0±1.9
			Late distal		
%^{45}Ca	95.0±0.2 (n = 11)	95.8±0.7 (n = 7; NS)		95.9±1.2 (n = 5; NS)	95.2±0.5 (n = 5; NS)
%[^{3}H]inulin	97.5±0.2	100.4±1.6		96.3±1.6	99.8±0.2

Values are means ± SE. Microinjections of ^{45}Ca and [^{3}H]inulin into early proximal, late proximal, early distal, and late distal tubules of Wistar rats were performed in control condition (10 rats) and in the presence of Gd^{3+} (4 rats), La^{3+} (4 rats), Cd^{2+} (7 rats), and nifedipine (3 rats). Early proximal data represent the percentage of excreted ^{45}Ca after microinjections in early proximal tubules, which reflect ^{45}Ca reabsorption in all the downstream segments after early proximal (proximal tubule, loop of Henle, distal tubule, and terminal segments). Late proximal data resulting from late proximal microinjections reflect ^{45}Ca reabsorption in all the downstream segments after late proximal (loop of Henle, distal tubule, and terminal segments). Early distal data reflect ^{45}Ca reabsorption along distal and terminal segments, and late distal data reflect ^{45}Ca reabsorption along terminal segments. [^{3}H]inulin and ^{45}Ca urine recoveries are expressed as the percentage of the injected amounts. The nos. (n) of microinjections and the P values are in parentheses. P values refer to the difference in the ^{45}Ca urine recoveries between control and experimental group. NS, not significant (Student's t-test).

an acute Cd loading. To be consistent with clearance and microinjection experiments, total plasma concentration of Cd^{2+} was maintained at 5 μM throughout the experiments. Under these conditions, the estimated ultrafiltrable plasma Cd concentration was 2.8 ± 0.2 μM (n = 7). Flow rate and single-nephron glomerular filtration were 34 ± 9 and 38 ± 4 nl/min (n = 7), respectively. The fractional delivery of Cd at the end of the accessible proximal tubule was 14.6 ± 1.4% (n = 7). Thus most of the 85% of the filtered Cd^{2+} was reabsorbed between the glomerulus and the late proximal tubule.

DISCUSSION

The aim of this study was to investigate specifically the transport of free Cd^{2+} in each segment of the nephron and to identify the putative transporters involved in the renal transport of Cd^{2+}. First, it was important to check the effect of acute Cd^{2+} intoxication on renal function. To do this, clearance experiments were carried out and infusion of $CdCl_2$ increased plasma free Cd^{2+} concentration to 3.03 ± 0.32 μM. Such a Cd^{2+} concentration corresponds to a 90 μg/kg body wt, equivalent to a low dose of acute Cd^{2+} intoxication (21). During Cd^{2+} infusion, GFR remained stable, indicating that glomerular function was unaffected. This is in agreement with light microscopy studies by Uriu et al. (31) showing that a single intraperitoneal dose of 0.4 mg/kg Cd^{2+} did not cause any identifiable glomerular pathology. Acute infusion of Cd^{2+} was associated with an increase in urine flow rate, a significant increase in FE of all the ions measured, and a parallel decrease in their plasma concentrations. The rapid and excessive renal losses of PO_4^{-2}, Na^+, K^+, Mg^{2+}, Ca^{2+}, and water were probably due to an effect of Cd^{2+} mainly on the proximal tubule, and the fall in plasma ion concentrations probably relates to this. Thus, although Cd^{2+} is already known to cause a Fanconi-like wasting of many solutes normally reabsorbed by

Table 2. *Unidirectional ^{45}Ca fluxes along the nephron*

	Control	+Cadmium	+Gadolinium	+Lanthanum	+Nifedipine
Proximal convoluted tubule	3.3%	3.6%	3.5%	2.3%	2.6%
Loop of Henle	66.1%	71.8%	81.4%	73.5%	61.9%
Distal convoluted tubule	22.2%	6.3%	4.1%	11.6%	23.8%
Terminal segment (CNT, CCT)	5.0%	4.2%		4.1%	4.8%

For each group, the difference between ^{45}Ca recovery after late proximal and early proximal injections (indicated in Table 1) gives the ^{45}Ca reabsorption in proximal convoluted tubule (PCT). CNT, connecting tubule; CCT, cortical convoluted tubule. ^{45}Ca reabsorption in the loop is obtained by difference between ^{45}Ca recovery after early distal and late proximal injections. Results are expressed as percentage of delivered load.

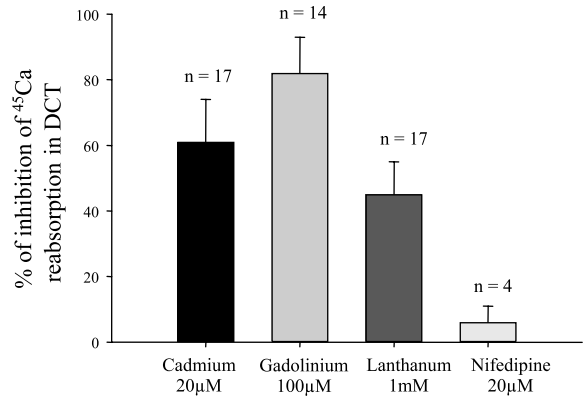

Fig. 4. Inhibitory effect of Cd (20 μM), Gd^{3+} (100 μM), La^{3+} (1 mM), and nifedipine (20 μM) on Ca^{2+} reabsorption in terminal part of the nephron. Percentages of inhibition were calculated from ^{45}Ca microinjection in early distal tubule. The nos. of microinjections are above each bar.

American Journal of Physiology – Renal Physiology

Downloaded from ajprenal.physiology.org on September 8, 2005

Table 3. *^{109}Cd recovery in urine after microinjection along the nephron*

	Control	+Gadolinium (90 μM)	+Iron (100 μM)	+Cobalt (100 μM)	+Bumetanide (50 μM)	+Zinc (50 μM)	+Zinc (500 μM)
				Early proximal			
%^{109}Cd	5.1±0.9	24.1±1.5	36.7±3.6	58.6±2.0	4.4±0.7	3.1±1.5	14.3±2.0
	(n = 18)	(n = 22; P<0.001)	(n = 9; P<0.001)	(n = 12; P<0.001)	(n = 22; NS)	(n = 16; NS)	(n = 17; P<0.001)
%[^{3}H]inulin	96.0±1.2	97.9±0.8	97.6±1.6	99.3±0.2	99.8±0.1	98.9±0.5	99.7±0.2
				Late proximal			
%^{109}Cd	14.9±1.6	47.9±5.9	63.5±8.6	70.2±4.9	62.7±2.1	12.0±8.3	28.2±5.1
	(n = 16)	(n = 11; P<0.001)	(n = 5; P<0.001)	(n = 14; P<0.001)	(n = 7; P<0.001)	(n = 2; NS)	(n = 8; P<0.02)
%[^{3}H]inulin	94.0±2.6	98.0±1.2	99.6±0.4	98.4±1.1	98.8±0.8	98.5±1.5	98.4±0.9
				Early distal			
%^{109}Cd	61.7±5.0	91.2±1.4	88.9±3.6	94.2±0.8	71.5±0.0	92.6±1.9	93.5±2.0
	(n = 20)	(n = 18; P<0.001)	(n = 5; P<0.001)	(n = 11; P<0.001)	(n = 1; NS)	(n = 8; P<0.001)	(n = 9; P<0.001)
%[^{3}H]inulin	100.5±1.3	99.0±0.5	99.2±0.7	98.2±1.0	100.0±0.0	99.1±0.9	99.7±0.2
				Late distal			
%^{109}Cd	86.0±1.8						
	(n = 4)						
%[^{3}H]inulin	100.0±0.0						

Values are means ± SE. Microinjections of ^{109}Cd and [^{3}H]inulin into early proximal, late proximal, early distal, and late distal tubules of Wistar rats were performed in control condition (7 rats) and in the presence of Gd^{3+} (10 rats), iron (5 rats), cobalt (4 rats), bumetanide (2 rats), and zinc (6 rats). As in Table 1, tracer amount in the urine reflects reabsorption of the tracer in all the downstream segments of the nephron. [^{3}H]inulin and ^{109}Cd urine recoveries are expressed as percentage of the injected amounts. The nos. (n) of microinjections and the P values are in parentheses. P values refer to the difference in the ^{109}Cd urine recoveries between control and experimental group (Student's t-test).

the proximal tubule (30), this is the first study to show that acute injection of Cd^{2+} can produce a Fanconi-like pattern of ion excretion. In the TAL segment of the LH, Cd^{2+} could reduce reabsorption by blocking ROMK channels (22). An effect on K^+ recycling in the apical membrane might account for reduced Na^+ and K^+ reabsorption, as well a decrease in paracellular transport of divalent cations. A dysfunction of the terminal segments of the nephron could also be involved in Cd^{2+}-induced salt wasting. In the DT, Ca^{2+} transport occurs via a transcellular pathway (3). Recently, many experiments have confirmed the involvement of the ECaC ion channel in Ca^{2+} reabsorption in the DT. In heterologous expression systems, ECaC generates Ca^{2+} currents inhibited by several divalent cations with a blocking order of $Gd^{3+} >> Cd^{2+} > La^{3+}$ and also slightly by L-type voltage-dependent Ca^{2+} channel antagonists/agonists (25, 32). In the present study, the unidirectional flux of ^{45}Ca estimated by microinjection in the DT shared the known pharmacological properties of ECaC. This suggests that ECaC might be the main transporter involved in distal reabsorption of Ca^{2+} and highlights a functional role for ECaC in the kidney. Another important finding was the nature of the distal Ca^{2+} transport inhibition induced by Cd^{2+}. Under diuretic conditions, the Ca^{2+} concentration at the beginning of the DT ranged between 0.5 and 1 mM. The fact that only 20 μM Cd^{2+} was sufficient to inhibit >60% of Ca^{2+} reabsorption indicates that Cd^{2+} acted as a channel blocker and did not compete directly with Ca^{2+} on the transporter. This observation corroborates the hypothesis of Peng et al. (25), who proposed an inhibition of ECaC via a binding of Cd^{2+} to a high-affinity inhibitory site. Thus inhibition of distal Ca^{2+} reabsorption by Cd^{2+} could explain the hypercalciuria elicited by acute intoxication.

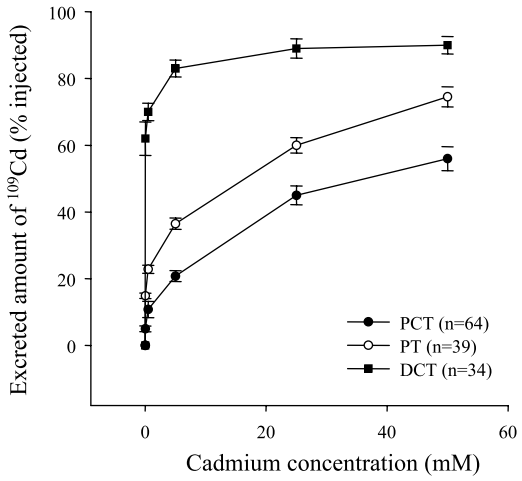

Fig. 5. Influence of Cd^{2+} concentration on urine excretion of ^{109}Cd after microinjection in early (PT) and late proximal (PCT) tubule and late distal tubule (DCT). Cd^{2+} concentrations were increased from 5 μM to 50 mM. ^{109}Cd excreted amounts are expressed in % of injected amount. The number of microinjections is in parentheses.

In contrast to Ca^{2+}, renal handling of Cd^{2+} is not well understood. Cd is an environmental pollutant, and its presence in tissues and biological fluids usually results from industrial contamination. The ^{109}Cd microinjections performed in the presence of various Cd^{2+} concentrations (ranging from 5 μM to 50 mM) indicate that the proximal tubule exhibits the highest reabsorptive capacity for Cd^{2+}. These results were corroborated by micropuncture data demonstrating that filtered Cd^{2+} is strongly reabsorbed by the early proximal tubule and that very little Cd^{2+} is delivered to the downstream segments (S3, LH, DT). Therefore, the difference between ^{109}Cd urinary recovery after late and early proximal microinjection did not reflect the ^{109}Cd transport between these two sites. The urinary recovery after early proximal microinjection probably corresponds to a best estimate of proximal transport. Finally, the present results indicated that 95% of Cd^{2+} was taken up by the

American Journal of Physiology – Renal Physiology

Downloaded from ajprenal.physiology.org on September 8, 2005

Table 4. *^{65}Zn recovery in urine after microinjection along the nephron*

	Control	+Cadmium (50 μM)
	Early proximal	
%^{65}Zn	14.3±4.3 (n = 7)	24.1±2.8 (n = 7)
%[^{3}H]inulin	98.4±10.6	97.4±4.5
	Medium proximal	
%^{65}Zn	30.1±2.9 (n = 7)	40.3±2.4 (n = 4)
%[^{3}H]inulin	97.9±8.2	99.8±5.7
	Late proximal	
%^{65}Zn	40.9±3.6 (n = 8)	48.4±4.1 (n = 4)
%[^{3}H]inulin	97.2±5.8	99.5±4.1
	Early distal	
%^{65}Zn	84.7±2.9 (n = 8)	99.3±0.9 (n = 4)
%[^{3}H]inulin	98.4±5.3	99.6±5.0

Values are means ± SE. Microinjections of ^{65}Zn and [^{3}H] inulin into early proximal, medium proximal, late proximal and early distal tubules of Wistar rats (8 rats) and in the presence of Cd^{2+} (5 rats) were performed. As in Tables 1 and 3, tracer amount in the urine reflects reabsorption of the tracer in all the downstream segments of the nephron. [^{3}H]inulin and ^{65}Zn urine recoveries are expressed as the percentage of the injected amounts. The nos. (n) of microinjections are in parentheses.

proximal tubule. Using a similar microinjection technique, Felley-Bosco and Diezi (8) calculated that 70% of injected inorganic Cd^{2+} was reabsorbed in the proximal tubule. Taken together, these data underline the important role of the proximal tubule in free Cd^{2+} reabsorption.

If we accept that Cd^{2+} is almost completely reabsorbed along the proximal tubule, the inhibition of Cd^{2+} transport in downstream segments should not affect the percentage of excreted ^{109}Cd after proximal injection. This is the case, because the presence of bumetanide (50 μM) or zinc (50 μM) did not change the percentage of Cd^{2+} recovered in the urine. Finally, although they exhibited permeability to Cd^{2+}, the segments beyond the proximal tubule did not significantly participate in Cd^{2+} transport at least at low Cd^{2+} concentrations. It is different at high Cd^{2+} concentrations and in the presence of factors that decrease proximal reabsorption of Cd^{2+}. The studies performed with Fe^{2+} (100 μM), Co^{2+} (100 μM), and Zn^{2+} (500 μM) revealed an inhibitory effect of these metals in the proximal tubule. Consequently, a significant amount of Cd^{2+} is delivered to the S3 segment, the LH, and terminal parts of the nephron, and the contribution of these segments to Cd^{2+} reabsorption then becomes significant.

The observation that Fe^{2+} and Co^{2+} clearly decrease Cd^{2+} transport in all segments suggests that the divalent metal cation transporter DMT1 is involved in the transcellular pathway. DMT1 can transport Fe^{2+}, Zn^{2+}, Mn^{2+}, Co^{2+}, Cd^{2+}, Cu^{2+}, Ni^{2+}, and Pb^{2+} (17) and has been localized to the proximal S3 segment, the LH, the DCT, and collecting ducts (10). In the proximal tubule, DMT1 is probably present in the endosomal compartment (10), whereas in downstream nephron segments it is located in the apical plasma membrane. Interestingly, Fe^{2+} and Co^{2+}, and a high concentration of Zn^{2+}, decreased proximal Cd^{2+} reabsorption, indicating that DMT1 might be involved in its transport. This result is different from the finding of Ferguson et al. (10) that DMT1 was not involved in the translocation of Fe^{2+} across the brush-border membrane of the proximal tubule. Actually, the transport systems involved in proximal reabsorption of Cd^{2+} remain unclear. However, the transporters belonging to the zinc-related transport-like protein (ZIP) family are possible candidates. Mouse ZIP1 is expressed in kidney tissue and located in the plasma membrane (6). Several other metals, such as Cd^{2+}, Fe^{2+} Co^{2+}, or Cu^{2+} inhibit Zn^{2+} uptake by this protein (6). It is tempting to speculate that a ZIP transporter might be involved in the transport of Zn^{2+} and Cd^{2+} along the proximal tubule. The blocking effect of Gd^{3+} indicates that stretch-activated cation channels could be also involved in Cd^{2+} uptake in the proximal tubule. However, the absence of the effect of Gd^{3+} on proximal ^{45}Ca transport suggests that stretch-activated cation channels play only a minor role in both Ca^{2+} and Cd^{2+} transport.

The present study demonstrated that Fe^{2+} and Co^{2+} decreased Cd^{2+} transport in segments downstream to the proximal tubule. Using microperfusion of ^{55}Fe, Wareing et al. (34) demonstrated significant reabsorption of Fe^{2+} in the LH and that this reabsorption could be mediated by DMT1 (10, 34). Thus it is reasonable to conclude that, like with Fe^{2+}, Cd^{2+} is transported, at least in part, by DMT1 in the apical membrane of the LH, in its TAL segment where DMT1 has been shown to be present (10).

In the LH and terminal nephron segments, ^{109}Cd microinjections in the presence of bumetanide highlight the role of a different pathway from the transcellular route for Cd^{2+} transport. In the TAL, the paracellular pathway plays an important role in divalent cation reabsorption. Bumetanide, by inhibiting Na^{+}-K^{+}-$2Cl^{-}$ cotransport, decreases the transepithelial voltage and diminishes cation paracellular reabsorption (5, 16). The fact that this loop diuretic decreased Cd^{2+} transport along LH and DT indicates that in these segments Cd^{2+} transport may also occur via the paracellular pathway.

The inhibitory effect of Gd^{3+} on ^{109}Cd and ^{45}Ca uptake suggests that Cd^{2+} might be reabsorbed through Ca^{2+} channels. ECaC could be one of these channels, because it participates in distal Ca^{2+} transport and it is blocked by low Cd^{2+} concentrations.

Using cells derived from distal portions of the nephron, Friedman and Gesek (11) have proposed that Cd^{2+} transport involves Ca^{2+} channels and a membrane transport protein that can be inhibited by Fe^{2+}. In light of more recent experiments, it is likely that this membrane transporter is DMT1 (11). Our data also support this conclusion, because distal Cd^{2+} permeability was strongly blocked by Fe^{2+}, Co^{2+}, and Zn^{2+}.

As far as zinc transport is concerned, the present study shows that Zn^{2+} is transported along the proximal tubule, the LH, and the terminal segments of the nephron. The finding that a low Zn^{2+} concentration (50 μM) did not modify Cd^{2+} transport in the proximal tubule and LH strongly suggests that Zn^{2+} and Cd^{2+} do not share the same uptake pathways in these segments. In the proximal tubule, Zn^{2+} could be transported in the apical membrane as a free ion via a saturable carrier-mediated process and an unsaturable pathway, or complexed with histidine or cysteine via a sodium-amino acid cotransport mechanism (12); however, the interaction of Cd^{2+} with such processes is unclear. In the LH, the lack of competition between Zn and Cd is perhaps surprising, because DMT1 has a strong affinity for Zn^{2+} (17) and may be one of the Cd^{2+} transporters in this segment. However, studies of Fe^{2+} transport by DMT1 in this segment by Wareing et al. (34) have

American Journal of Physiology – Renal Physiology

Downloaded from ajprenal.physiology.org on September 8, 2005

shown a lack of competition between Zn^{2+} and Fe^{2+}. According to these authors, it is possible that in the LH, DMT1 does not transport Zn^{2+}, or transports it with only low efficiency. This possibility is consistent with our data, because a high Zn^{2+} concentration (500 μM) only produced a modest decrease in Cd^{2+} absorption along the LH.

Along the terminal nephron segments, Zn^{2+} inhibited Cd^{2+} transport and vice versa, suggesting that DMT1 may play an important role in Zn^{2+} reabsorption in this part of the nephron. Interestingly, four DMT1 isoforms have been identified in renal tissue (19). Thus the difference between the effects of Zn^{2+} action on Cd^{2+} uptake in the LH and more distal segments could be due to the pattern of expression of these different isoforms (33).

The results obtained in the present study suggest several ways in which Cd^{2+} might be eliminated: *1*) in the proximal tubule by blocking paracellular and transcellular pathways (unknown for the moment); *2*) in the LH by use of loop diuretics (such as bumetanide and furosemide) and DMT1 inhibition; and *3*) in the distal tubule by DMT1 inhibition. Our findings on Cd^{2+} transport highlight the need to characterize the properties in vivo of these different transport pathways and to develop pharmacological tools with which to manipulate DMT1 function.

ACKNOWLEDGMENTS

We are grateful to Dr. Robert Unwin for constructive criticism of this manuscript, corrections and for helpful discussions.

REFERENCES

1. **Ahn DW, Kim YM, Kim KR, and Park YS.** Cadmium binding and sodium-dependent solute transport in renal brush-border membrane vesicles. *Toxicol Appl Pharmacol* 154: 212–218, 1999.
2. **Aughey E, Fell GS, Scott R, and Black M.** Histopathology of early effects of oral Cd in the rat kidney. *Environ Health Perspect* 54: 153–161, 1984.
3. **Bindels RJ.** Calcium handling by the mammalian kidney. *J Exp Biol* 184: 89–104, 1993.
4. **Brzoska MM, Kaminski M, Supernak-Bobko D, Zwierz K, and Moniuszko-Jakoniuk J.** Changes in the structure and function of the kidney of rats chronically exposed to Cd. I. Biochemical and histopathological studies. *Arch Toxicol* 77: 344–352, 2003.
5. **Burg M, Stoner L, Cardinal J, and Green N.** Furosemide effect on isolated perfused tubules. *Am J Physiol* 225: 119–124, 1973.
6. **Dufner-Beattie J, Langmade SJ, Wang F, Eide D, and Andrews GK.** Structure, function, and regulation of a subfamily of mouse zinc transporter genes. *J Biol Chem*. Manuscript M304163200, October 2003.
7. **Erfurt C, Roussa E, and Thevenod F.** Apoptosis by Cd^{2+} or CdMT in proximal tubule cells: different uptake routes and permissive role of endo/lysosomal CdMT uptake. *Am J Physiol Cell Physiol* 285: C1367–C1376, 2003.
8. **Felley-Bosco E and Diezi J.** Fate of Cd in rat renal tubules: a microinjection study. *Toxicol Appl Pharmacol* 91: 204–211, 1987.
9. **Felley-Bosco E and Diezi J.** Fate of Cd in rat renal tubules: a micropuncture study. *Toxicol Appl Pharmacol* 98: 243–251, 1989.
10. **Ferguson CJ, Wareing M, Ward DT, Green R, Smith CP, and Riccardi D.** Cellular localization of divalent metal transporter DMT-1 in rat kidney. *Am J Physiol Renal Physiol* 280: F803–F814, 2001.
11. **Friedman PA and Gesek FA.** Cadmium uptake by kidney distal convoluted tubule cells. *Toxicol Appl Pharmacol* 128: 257–263, 1994.
12. **Gachot B, Tauc M, Morat L, and Poujeol P.** Zinc uptake by proximal cells isolated from rabbit kidney: effects of cysteine and histidine. *Pflügers Arch* 419: 583–587, 1991.
13. **Gennari A, Cortese E, Boveri M, Casado J, and Prieto P.** Sensitive endpoints for evaluating Cd-induced acute toxicity in LLC-PK1 cells. *Toxicology* 183: 211–220, 2003.
14. **Gottschalk CW and Mylle M.** Micropuncture study of pressures in proximal tubules and peritubular capillaries of the rat kidney and their relation to ureteral and renal venous pressures. *Am J Physiol* 185: 430–439, 1956.
15. **Goyer RA and Cherian MG** (Editors). *Toxicology of Metals: Biochemical Aspects. Handbook of Experimental Pharmacology*. New York: Springer-Verlag, 1995, vol.115, p. 189–213.
16. **Greger R, Oberleithner H, Schlatter E, Cassola AC, and Weidtke C.** Chloride activity in cells of isolated perfused cortical thick ascending limbs of rabbit kidney. *Pflügers Arch* 399: 29–34, 1983.
17. **Gunshin H, Mackenzie B, Berger UV, Gunshin Y, Romero MF, Boron WF, Nussberger S, Gollan JL, and Hediger MA.** Cloning and characterization of a mammalian proton-coupled metal-ion transporter. *Nature* 31: 482–488, 1997.
18. **Herak-Kramberger CM, Spindler B, Biber J, Murer H, and Sabolic I.** Renal type II Na/P_i-cotransporter is strongly impaired whereas the Na/sulphate-cotransporter and aquaporin 1 are unchanged in Cd-treated rats. *Pflügers Arch* 432: 336–344, 1996.
19. **Hubert N and Hentze MW.** Previously uncharacterized isoforms of divalent metal transporter (DMT)-1: implications for regulation and cellular function. *Proc Natl Acad Sci USA* 99: 12345–12350, 2002.
20. **Lechene C, Morel F, Guinnebault M, and De Rouffignac C.** Micropuncture study of urine formation. I. In the rat during various diuretic states. *Nephron* 6: 457–477, 1969.
21. **Liu J, Habeebu SS, Liu Y, and Klaassen CD.** Acute CdMT injection is not a good model to study chronic Cd nephropathy: comparison of chronic $CdCl_2$ and CdMT exposure with acute CdMT injection in rats. *Toxicol Appl Pharmacol* 153: 48–58, 1998.
22. **Loussouarn G, Makhina EN, Rose T, and Nichols CG.** Structure and dynamics of the pore of inwardly rectifying K_{ATP} channels. *J Biol Chem* 275: 1137–1144, 2000.
23. **Ma R, Smith S, Child A, Carmines PK, and Sansom SC.** Store-operated Ca^{2+} channels in human glomerular mesangial cells. *Am J Physiol Renal Physiol* 278: F954–F961, 2000.
24. **Markovich D and Knight D.** Renal Na-Si cotransporter NaSi-1 is inhibited by heavy metals. *Am J Physiol Renal Physiol* 274: F283–F289, 1998.
25. **Peng JB, Chen XZ, Berger UV, Vassilev PM, Brown EM, and Hediger MA.** A rat kidney-specific Ca transporter in the distal nephron. *J Biol Chem* 275: 28186–28194, 2000.
26. **Prozialeck WC, Lamar PC, and Lynch SM.** Cadmium alters the localization of N-cadherin, E-cadherin, and beta-catenin in the proximal tubule epithelium. *Toxicol Appl Pharmacol* 189: 180–195, 2003.
27. **Robinson MK, Barfuss DW, and Zalups RK.** Cadmium transport and toxicity in isolated perfused segments of the renal proximal tubule. *Toxicol Appl Pharmacol* 121: 103–111, 1993.
28. **Savolainen H.** Cadmium-associated renal disease. *Ren Fail* 17: 483–487, 1995.
29. **Takebayashi S, Jimi S, Segawa M, and Kiyoshi Y.** Cadmium induces osteomalacia mediated by proximal tubular atrophy and disturbances of phosphate reabsorption. A study of 11 autopsies. *Pathol Res Pract* 196: 653–663, 2000.
30. **Thevenod F.** Nephrotoxicity and the proximal tubule. Insights from Cd. *Nephron Physiol* 93: 87–93, 2003.
31. **Uriu K, Kaizu K, Komine N, Ikeda M, Qie YL, Hashimoto O, Matsuoka A, and Eto S.** Renal hemodynamics in rats with Cd-induced nephropathy. *Toxicol Appl Pharmacol* 150: 76–85, 1998.
32. **Vennekens R, Prenen J, Hoenderop JG, Bindels RJ, Droogmans G, and Nilius B.** Pore properties and ionic block of the rabbit epithelial Ca channel expressed in HEK 293 cells. *J Physiol* 530: 183–191, 2001.
33. **Wareing M, Ferguson CJ, Delannoy M, Cox AG, McMahon RF, Green R, Riccardi D, and Smith CP.** Altered dietary iron intake is a strong modulator of renal DMT1 expression. *Am J Physiol Renal Physiol* 285: F1050–F1059, 2003.
34. **Wareing M, Ferguson CJ, Green R, Riccardi D, and Smith CP.** In vivo characterization of renal iron transport in the anaesthetized rat. *J Physiol* 524: 581–586, 2000.

American Journal of Physiology – Renal Physiology

Downloaded from ajprenal.physiology.org on September 8, 2005